Figure 5.21: A schematic diagram of readout electronics for the beam-beam counter.

a magnetic shield. A thin metal attachment, with three tapped holes and an opening at the center for a laser pulse fiber, is glued to the front face of the radiator with epoxy resin.

Each of the 66 identical elements is mounted on a base plate with three screws, then an optical fiber is plugged into the optical coupler for each counter. A rear plate attaches with bolts to the front base plate, as shown in the center part of Fig. 5.20. On the rear plate, high voltage distributors and signal patch-panels are mounted. The entire assembly, including the front and rear plates must separate into two sectors to fit around the beam pipe. Each half assembly is covered with a thin metal jacket. The front and rear plates may be cooled by cooling water. The assemblies can slide into the copper plug on the muon spectrometer side, as shown in the bottom of Fig. 5.20, and the front plate is fixed with bolts to the plug. An identical assembly is mounted on a stand on the other side.

Access to the beam-beam counter assembly on the muon spectrometer side is possible as the copper plug actually consists of three parts. The section further downstream of the beam-beam counter is fabricated as one cylindrical part and slides into the muon tracking region. The section around the beam-beam counter consists of two parts, and the upper part is removable to expose the beam-beam counter assembly. This can then be removed, one half-assembly at a time. Nevertheless, access to the counter inside the plug is not easy. Because of this, and the large number of neutrons inside the plug, we show the front-end and readout electronics outside the copper plug. Consequently, 66 coaxial signal cables and nine high-voltage cables are laid through an opening in the plug, and 66 optical fiber cables enter the beam-beam array through the front of the plug.

## 5.11 Electronics

The BB electronics chain, shown in Fig. 5.21, consists of discriminators, shaping amplifiers, time-to-amplitude converters (TAC), flash ADCs (FADC) and buffer memories. We use electronics which are common with the TOF system wherever possible. However, there are some differences due to the dynamic range required of the BB elements, and the timing requirements driven by the beam crossing time.

### 5.11.1 Front-end

The signal from each element of BB is split three ways. One goes to a discriminator and time-to-amplitude converter (TAC), to generate the timing measurement. In central Au + Au collisions, each element is likely to be hit by multiple particles. The timing signal arises from the first particle or particles entering the element, but the measured pulse height includes all particles, so a traditional slewing correction is impossible to apply. We will address this problem by using a constant fraction discriminator (CFD). There are two potential candidates for this discriminator. One is a conventional NIM standard constant fraction discriminator, and the other is mounted in the photomultiplier tube base, that is, an "on-tube" discriminator. The spatial volume for the BB installation is rather limited, and the radiation level is expected to be high, particularly inside the copper plug on the muon side. Consequently, the readout electronics resides outside of the plug. In this case, conventional NIM discriminator modules are preferable for reasons of stability and accessibility.

### 5.11.2 Readout and Trigger Interface

The readout electronics provides digitized time information for the LVL-1 trigger, and keeps timing and pulse height information in buffer memories for the data acquisition system. To record the timing information with good precision (25 ps/channel) and cover a reasonable range of time (about 20 ns), 10-bit FADCs are used to digitize the timing information. The TAC must also have adequate gain and resolution to achieve the 25-ps resolution. To provide an good vertex position in the LVL-1 trigger, time offsets of the BB modules must be corrected in the readout chain. This can be done by subtracting timing offsets using a lookup table after the FADCs.

In a central Au + Au collision the average number of particles entering a BB element is approximately 10. As the signal from a single particle hitting a module should also be recorded, a large dynamic range is necessary. To provide a sufficient dynamic range for the pulse heights, both low and high gain shaping amplifiers are used. The output of each goes to an individual FADC. Ten-bit resolution is adequate to record the pulse height information in such an arrangement.

### 5.11.3 Performance

Although a central Au + Au collision puts about 10 particles into the typical BB element, in a p + p collision, it is more likely that there will be only one or two particles in an entire array. This implies a large dynamic range in the electronics, but also a large variation in the amount of light collected per element. Nevertheless, the timing requirements are equally stringent in the high and low multiplicity cases.

The interaction position along the beam axis will be calculated from individual time measurements of fast leading particles hitting BB on the both sides of the interaction point.

With an intrinsic timing resolution of 70 ps, BB determines the interaction position with a precision of approximately 2 cm. This information is available to the LVL-1 as well as offline. The beam tests described in Appendix B show that such resolutions can certainly be achieved with the type of BB elements we have designed. The intrinsinc timing resolution measured with 1.6 GeV/c pions is 44 ps.

In addition to the prompt particles, there are also slower particles entering the BB elements. These are not useful for the precise interaction time as their velocities and flight paths are not known, and they represent a background. Another background source is the thermal noise in the BB elements. To reject background signals which fire discriminators randomly or in a period immediately after the arrival of the prompt particles, we derive the interaction time only from particles arriving within 10–20 ps of the beam crossing time. Accordingly, the relative timing of each counter element in the array has to be adjusted to this accuracy. During data taking, time drifts of each counter element will be monitored on-line with a laser calibration system, However, the long-term timing resolution is unlikely to reach the ideal intrinsic resolution values as timing drifts with temperature and over long periods of time are difficult to correct perfectly even with careful monitoring. We have therefore designed a system to achieve an intrinsic timing resolution, after slewing corrections, of 50 ps in tests of prototype counter elements.

### 5.11.4 Background in Environment of Beam-beam Counters

Background simulations were done with LAHET for the beam-beam counters, with particular attention paid to the production of neutrons by the copper plug surrounding the beam-beam counter on the muon side. There is some production of secondary (soft) charged particles from showers in the plug material, but these do not dominate the charged particle spectrum. These soft hadrons should not produce cerenkov light in the beam-beam counter elements, so will not produce a significant background to the measurement. The number of secondaries is sufficiently low that they do not create a radiation damage problem. Of more concern is the production of neutrons both from the magnet yoke (affecting both beam-beam counters) and by particles hitting the copper plug. The simulations show a neutron flux of 7 x $10^{11}$ per $cm^2$ per RHIC year on the beam-beam counter opposite the muon arm, and 3 x $10^{12}$ on the muon side. There is a potential for neutron-induced radiation damage in the beam-beam counter materials, particularly on the muon arm side. This implies a careful choice of materials used, such as the optical cement for assembly of radiator and photomultiplier tube. Furthermore, we will investigate the properties of the photocathode we intend to use under such neutron doses. The radiation environment is one of the factors driving the decision to locate the electronics outside of the beam-beam counter assembly.

## 5.12 Cost

The cost estimate for the beam-beam counter subsystem is broken down by WBS item and is given in Table 5.6. presented below.

Table 5.6: Cost Estimate for the PHENIX BB Counters

| | | Amounts in FY93 k$ | | | |
|---|---|---|---|---|---|
| W B S | Description | Total | M&S | EDIA | Labor |
| **5. 2.** | **Beam-Beam Counter** | **361** | **300** | **37** | **25** |
| **5. 2. 2** | **Beam-Beam Detector** | **299** | **267** | **13** | **20** |
| 5. 2. 2. 0 | EDIA | 13 | 0 | 13 | 0 |
| 5. 2. 2. 1 | Prototypes | 17 | 17 | 0 | 0 |
| 5. 2. 2. 2 | Fabrication | 265 | 250 | 0 | 15 |
| 5. 2. 2. 3 | Testing | 0 | 0 | 0 | 0 |
| 5. 2. 2. 4 | Installation | 5 | 0 | 0 | 5 |
| **5 8 1. 2. 2** | **Beam-Beam Electronics** | **62** | **33** | **24** | **5** |
| 5 8 1. 2. 2. 0 | EDIA | 24 | 0 | 24 | 0 |
| 5 8 1. 2. 2. 1 | Prototypes | 8 | 8 | 0 | 0 |
| 5 8 1. 2. 2. 2 | Fabrication | 25 | 25 | 0 | 0 |
| 5 8 1. 2. 2. 3 | Testing | 5 | 0 | 0 | 5 |

## 5.13 Schedule

The schedule for the beam-beam counters is shown below. In 1993, we will carry out several tests of prototype counter elements to fix the design with minimum ionizing particle and with high energy heavy ion beams. We will also test radiation hardness of the prototype counters with gamma ray and neutron beam irradiations. In 1994, we will build and test a prototype counter array with about 10 counter elements. During these two years, R&D work on the laser calibration system and electronics design will also be completed. We plan to construct whole the system in Japan in Japanese fiscal years 1995 and 1996. At the end of 1996, we will ship the counter assembly to BNL, and install it in the PHENIX spectrometer. The installation will take only a few months, so the BB will be available for the commissioning and integrated PHENIX tests during most of 1997.

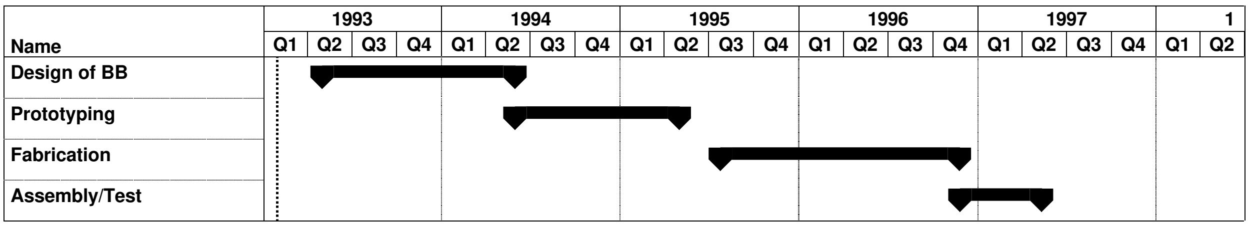


Figure 5.22: Overall schedule for the PHENIX BB counters.

# Bibliography


[1] SDC Technical Design Report, SDC-92-201, April 1992.

[2] "A Silicon Microvertex Detector for L3", SMD Study Group, L3-Internal Report #924 (April 19, 1991).

[3] C.L. Britton, Jr., G.T. Alley, M.L. Simpson, A.L. Wintenberg, R.J. Yarema, T. Zimmerman, J. Boissevain, J. Simon-Gillo, J.P. Sullivan, B.V. Jacak, and N. Lockyer, submitted to IEEE Nuclear Science Transactions.

[4] S. Ozaki, Nucl. Phys. **A525**, 125c (1991).

[5] W.C. Carithers, et al., Nucl. Inst. Meth. **A289**, 388, (1990).

[6] A. Bialas and R. Peschanski, Nucl. Phys. **B273**, 703 (1986); **B308**, 857 (1988).

[7] J. Kang, " Intermittency in Central Collisions of $^{16}$O + A at 14.6 A·GeV", E-802 Collaboration internal note (unpublished).

[8] T. Sugitate et.al., Nucl. Instr. and Meth. **A249**, 354 (1986).